

Antimicrobial, antioxidant, and angiogenic bioactive silver nanoparticles produced using *Murraya paniculata* (L.) jack leaves

Nanomaterials and Nanotechnology
Volume 12: 1–10
© The Author(s) 2022
Article reuse guidelines:
sagepub.com/journals-permissions
DOI: 10.1177/18479804211056167
journals.sagepub.com/home/nax


Purushothaman Rama¹, Alberto Baldelli² , Anandhan Vignesh¹, **Ammar B Altemimi³** , Govindan Lakshmanan^{1,4}, Rajendran Selvam⁴, Narasingam Arunagirinathan⁵, Kandasamy Murugesan¹ and Anubhav Pratap-Singh² 

Abstract

Murraya paniculata (MP) can be used as a reducing agent to produce silver nanoparticles (AgNPs) using a simple procedure. AgNPs are characterized in morphological and chemical properties, antioxidant activity, and cytotoxicity. The morphology of AgNPs derived from MP shows a face-centered cubic structure, spherical shape with an average particle size of 23 nm. The chemical structure shows characteristic peaks of AgNPs using UV-vis spectrometer at 438 nm. The formation of AgNPs is confirmed by analyzing their vibrational states under infrared radiation; typical peaks of AgNPs are recognized: at 3429 cm⁻¹ (O-H stretch, H-bonded alcohols, phenols groups), 2923 cm⁻¹ (C-H stretch alkanes), 1626 cm⁻¹ (N-H bend 1° amines), 1583 cm⁻¹ (C-C stretch in ring aromatic), 1039 cm⁻¹ (C-N stretch aliphatic amines), 728 cm⁻¹ (C-Cl stretch alkyl halides), and 589 cm⁻¹ (C-Br stretch alkyl halides), respectively. AgNPs produced from MP show antioxidant activity and cytotoxicity. They show the highest sensitivity toward *Bacillus cereus*. Cytotoxicity of biosynthesized AgNPs, determined by scratch wound assay on in vitro human endothelial vein cell, created from MP showed dose-dependent activity. These AgNPs, at a concentration of 15.625 µg/mL, stimulate the proliferation and migration of endothelial cells (EC) showing an angiogenic activity.

Keywords

Silver nanoparticles, *Murraya paniculata*, cytotoxicity, vascular endothelial growth factor

Date received: 19 May 2021; accepted: 11 October 2021

Topic Area: Nanoparticles and Colloids
Topic Editor: Raphael Schneider
Associate Editor: Lavinia Balan

Introduction

Nanotechnology is a research area in constant growth, and its application varies from electronics, biomedicine, environment, food, textile, and biomedicine.¹ Metallic nanoparticles are a large and important component of nanotechnology. High surface area, low melting point, and optical and magnetical properties are just some of the characteristics that make metal nanoparticles appealing in nanotechnology.^{2,3}

Silver nanoparticles (AgNPs) have attracted intensive research interest because of their advantageous applications,

¹Centre for Advanced Studies in Botany, Guindy Campus, University of Madras, Chennai, India

²Food Nutrition and Health Program, Faculty of Land and Food Systems, The University of British Columbia, Vancouver, Canada

³Food Sciences Department, University of Basrah, Basrah, Iraq

⁴Bharath Institute of Higher Education and Research, Chennai, India

⁵Meenakshi Academy of Higher Education and Research, Chennai, India

Corresponding author:

Anubhav Pratap-Singh, Food Nutrition and Health Program, Faculty of Land and Food Systems, The University of British Columbia, 2357 Main Mall, Vancouver V6T 1Z4, Canada.

Email: anubhav.singh@ubc.ca



Creative Commons CC BY: This article is distributed under the terms of the Creative Commons Attribution 4.0 License (<https://creativecommons.org/licenses/by/4.0/>) which permits any use, reproduction and distribution of the work without further permission provided the original work is attributed as specified on the SAGE and Open Access pages (<https://us.sagepub.com/en-us/nam/open-access-at-sage>).

not only in biomedical⁴ but also in drug delivery,⁵ food industries,⁶ agriculture,⁷ and textile industries.⁸ AgNPs show a unique antibacterial property; silver components are toxic to any microorganisms.⁹ It is well-known that cell death can be provoked by structural and morphological changes induced by AgNPs.⁹ Other typical properties of AgNPs are optical, thermal, and catalytic. When excited by a light source, a collective oscillation is generated on the conduction electrons on the surface. High thermal conductivity, high electrical conductivity, and high thermal stability are some of the thermal properties of AgNPs.¹⁰ High surface area is the main reason for the excellent catalytic properties of AgNPs and, similarly, to other types of nanoparticles.^{10,11} These characteristics are highly influenced by particle morphology and size.¹² High control over the morphological properties of final properties is achieved by employing chemical procedures that can have hidden dangerous side effects for human health.¹³ Several efforts are placed into developing green alternatives for the production of nanocomponents.^{14–17}

Biological methods of nanoparticles synthesis using microorganisms, enzymes, fungus, and plants have been suggested as alternatives to chemical and physical methods.¹ Plant-mediated nanoparticle synthesis is preferred as non-toxic, cost-effective, eco-friendly, and safe for human therapeutic use.¹⁸ Furthermore, the use of plant extracts to synthesize nanoparticles is advantageous over microorganisms due to the ease of scale-up, the less biohazard, and the elaborate process of maintaining cell cultures.¹⁹

Several plant extracts are present in literature references focused on synthesizing AgNPs.^{20,21} *Murraya paniculata* (Rutaceae) (*MP*) is a shrub commonly known as Orange Jasmine. It shows a broad spectrum of medicinal, pharmacological, and therapeutic properties.²² This plant is known to have antifertility,²³ antinociceptive and antiinflammatory,²⁴ antidiarrheal,²⁵ antidiabetic and antioxidant,²⁶ antianxiety,²⁷ and antibacterial²⁸ properties. Hence, we aim to synthesize and characterize AgNPs from *MP* to understand their possible future applications.

Materials and methods

Materials

AgNPs were synthesized from fresh leaves of *MP* aqueous extract; silver nitrate (AgNO_3) was purchased from Sigma Aldrich. Nutrient Agar (NA) and Muller Hilton Agar (MHA) were procured from HiMedia, and Dimethyl Sulfoxide (DMSO) from SD Fine-Chem Limited.

Preparation of *M. paniculata*

Fully-grown fresh leaves of *MP* were collected from Guindy campus, University of Madras. The collected fresh leaves were cleaned with running distilled water (DI) to remove the

dust particles. Around 8 grams of leaves were chopped and mixed with 100 mL of DI, and boiled in a microwave oven for 10 minutes. Then, the samples were allowed to cool at 20°C, and the extracts were filtered with Whatman No. 1 filter paper. Last, the aqueous crude extract was collected and stored at room temperature.

Synthesis of AgNPs

About 10 mL of aqueous extract of *MP* was incubated with AgNO_3 (1 mM) solution in an Erlenmeyer flask in a dark condition for 24 hours. The reaction mixture generated a change in color of the solution, from light green to dark brown, indicating the reduction of AgNPs.

Characterization of AgNPs

The reduction of pure silver Ag^+ ions was monitored by measuring the reaction mixture's UV-Vis spectrum at wavelength from 200 to 800 nm. Moreover, 1 mM AgNO_3 solution was used for the baseline correction. The morphology of the AgNPs was examined using a Field Emission Scanning Electron Microscope (HITACHI SU6600 FESEM) with Energy Dispersive Analysis X-Ray (EDAX). Thin films were prepared on aluminum foil by dropping a small portion of the sample (about 10 mL) and placed on a copper grid. For a nanoscale analysis, microscopes with a transmission mode are considered more appropriate.^{29–36} For HRTEM analysis, samples were sputter coated on a copper stub with a 20 nm layer of gold. TEM measurements were performed on instruments operated at an accelerating voltage of 200 kV. The formation and quality of the compounds were evaluated by XRD analysis using an XPERT-PRO with a diffractometer and with an operating voltage of 40 kV at a current strength of 30 mA. The samples were subjected to $\text{Cu K}\alpha$ radiation, and the scanning was done in the region of 30°–80°C. The images obtained were compared with the Joint committee on powder diffraction standards (JCPDS) library to account for the crystalline structure. To identify the biomolecules present within the AgNPs, FTIR analysis was performed with the KBr pellet in the range of 400–4000 cm^{-1} .

Screening of antimicrobial activity for silver nanoparticles

The antimicrobial effect of synthesized AgNPs was tested against a few human pathogens, such as Gram-positive *Bacillus cereus*, *Staphylococcus aureus*, Gram-negative *Escherichia coli*, and *Candida albicans* by well diffusion method. Active cultures for experiments were prepared by transferring a loop of the stock solution to the nutrient broth and incubated for 18 hours at 37°C. Each culture was swabbed uniformly into the individual nutrient agar plates

using sterile cotton swabs. A 6-mm-hole was bored aseptically with a sterile cork borer. Using a sterile micropipette, 100 μL of plant extract, AgNPs, and standard antibiotic ampicillin were loaded into well and it was allowed to dry. AgNO_3 (1 mM) was used as a control. After 24 hours of incubation, the diameter of the zone of inhibition was measured.³⁷

Antioxidant potential of AgNPs

DPPH radical scavenging activity. To assess the scavenging ability on 2,2-diphenyl-1-picrylhydrazyl (DPPH), 1 mL of DPPH (0.1 mM) was added to different concentrations (50, 100, 150, 200, and 250 $\mu\text{g}/\text{mL}$) of aqueous leaf extract and AgNPs.³⁸ The reaction mixture was shaken and incubated in dark for 30 minutes. The absorbance at 517 nm was measured using a UV-Visible spectrophotometer. Ascorbic acid was used as a standard. The lower absorbance of the reaction mixture indicated a higher percentage of scavenging activity. The percentage of inhibition or scavenging of radicals (RSA) was determined by equation (1), where A_{control} stays for the absorbance of the control and A_{sample} for the absorbance of the sample

$$RSA = \left(A_{\text{Control}} - \frac{A_{\text{Sample}}}{A_{\text{Control}}} \right) \times 100 \quad (1)$$

Reducing potential activity. The reducing power assay was conducted based on the method of Oyaizu (1986).³⁹ Different concentrations of aqueous extract (1 mL) and AgNPs were separately mixed with 2.5 mL of phosphate buffer (0.2 M pH 6.6) and 2.5 mL of potassium ferricyanide (1%). The mixture was incubated at 50°C for 20 minutes. To this mixture, 2.5 mL of trichloroacetic acid (10%) was added, which was then centrifuged at 3000 r/min for 10 minutes. Later, 2.5 mL of the supernatant solution was mixed with 2.5 mL of DI water and 0.5 mL of ferric chloride (0.01%). The absorbance was measured at 700 nm using a UV-Visible spectrophotometer.

Cytotoxicity of silver nanoparticles on human umbilical vein endothelial cell line

Cell line and drug preparation. The human umbilical vein endothelial cell line (HUVEC) was obtained from NCCS (National Centre for Cell Sciences), Pune, India. The cells were cultured in Dulbecco's Modified Eagle's Medium (DMEM) supplemented with 10% fetal bovine serum (Hi-media) and 2 mM glutamine (Sigma chemical co), 100 IU/ml penicillin, and 100 $\mu\text{g}/\text{mL}$ streptomycin (GIBCO BRL). The cells were maintained at 95% air humidity in a biological incubator at 37°C with 5% CO_2 ; then, the viability was assessed using MTT assay. The stock solution was

prepared in DMSO and was stored at -20°C until use. The concentrations used for the study were freshly prepared for each experiment with a final DMSO concentration of 0.1%.

Assessment of cell viability using MTT assay. The cell viability of the AgNPs from MP was determined by MTT assay (Mossman, 1983). HUVEC cell line was cultured and seeded in 96-well plates approximately (1×10^5 cells/well) was incubated for 24 hours at 95% air humidity in a biological incubator at 37°C with 5% CO_2 . Cells were replaced with fresh media containing different concentrations (from 3.925 to 1000 $\mu\text{g}/\text{mL}$) of synthesized AgNPs and incubated for 48 hours. Thereafter, the supernatant was removed and cells were washed with DMEM medium. Subsequently, these plates were subjected to MTT (3-(4, 5-dimethylthiazol-2-yl), 2,5-diphenyltetrazolium bromide, a yellow tetrazole) assay. MTT (10 μL) was added to each well and incubated overnight at 37°C. Purple formazone crystals were dissolved in 100 μL of DMSO. The suspensions were read at 570 nm using a spectrophotometer. The effect of the drug on growth is assessed as the percent of cell viability.

Cell migration analysis using AgNPs. The cell migration of HUVEC was evaluated using a scratch wound assay.⁴⁰ In brief, 1×10^5 cells/ml were added into 24-well culture plates and cultured overnight. The cells were starved with 1% v/v FBS medium for 24 hours. The cells were then scraped with a cross in the middle of the well with 200 μL pipette tips, and the medium was changed with a fresh medium containing IC_{50} concentration of AgNPs. The cells were then incubated for 48 hours. The cells around the wounds were visualized and imaged under an inverted microscope ($\times 4$ magnification). The percentages of the open wound areas were estimated under a microscope.

Expression of vascular endothelial growth factor using western blot analysis. The western blot analysis was carried out to detect VEGF expression on endothelial cells. HUVEC (1×10^5 cells/well) were seeded in a 24-well culture plate and incubated for 24 hours. Various concentrations (3.925–1000 $\mu\text{g}/\text{mL}$) of AgNPs were added to the well plates and incubated for 48 hours. After the treatment, cells were harvested and washed twice with PBS. The cell pellets were then lysed with RIPA buffer (50 mM Tris-HCl pH 7.4; 150 mM sodium chloride; 0.1% SDS; Triton-X-100; 5 mM EDTA; 0.25% sodium deoxycholate) for 15 minutes in ice. The samples were then centrifuged at 14,000 r/min for 5 minutes at 4°C. The protein concentrations were determined by Bicinchoninic acid (BCA) method. The supernatant protein was resolved by 12% SDS and transferred to 0.45 μM PVDF membranes (polyvinylidene fluoride). The membrane was then blocked with 5% non-fat milk in Tris-buffered saline containing Tween 20 (20 mM Tris-HCl pH 7.6; 150 mM NaCl; 0.1% Tween

20). The blots were incubated overnight with primary antibodies against human beta-actin (1:2000). After incubation with the secondary horseradish peroxidase-conjugated antibodies for 2^ohours, detection was performed using a chemiluminescence assay kit. The densities of the bands were evaluated using total lab software, and the signal was normalized for β -actin.

Statistical analysis

All data were expressed as mean and standard error derived by the repetition of each test at least three times. All the analyses were calculated using the Statistical Package of Social Sciences (SPSS) software package version 16.0 program using analysis of variance (ANOVA) to investigate the effect. Results with $p < 0.05$ were considered to be statistically significant.

Results and discussion

Properties characterization

AgNPs produced by several techniques and sources characterized by few main properties, such as morphology, chemical composition, crystallinity, and stability.¹⁴ Determining these properties estimates the quality of the AgNPs and their applicability to different purposes.

Stability. One of the most important properties of nanoparticles produced by a green procedure is stability. The easiest procedure to verify if in a solution AgNPs are present would be performing a visual check. It is well-known that the optical properties of spherical AgNPs depend on the AgNPs diameter and the refractive index near the nanoparticles.⁴¹ Moreover, unaggregated AgNPs usually show a yellow–orange color in the solution; however, when the particles aggregate, the color of the solution would appear grey.⁴² In our project, the AgNPs are formed by adding different concentrations of extracts (5^oml, 10^oml, 15^oml, and 20^oml) with aqueous AgNO₃ (1^omM). After 24^ohours incubation, the colors of the

solutions with different concentrations of MP and AgNO₃ vary from yellow to dark brown (Figure 1 (a)). Therefore, by selecting a variety of concentrations of both MP and AgNO₃, the nanoparticles do not show any sign of aggregation after a day of incubation. The grey tone is obtained only in case of a solution of a 100 weight percent of AgNO₃, when no AgNPs are formed.

For the solution containing 10^oml of MP extract, the AgNPs appear very stable even after 30^odays. The UV spectrum does not show major alterations from one to 30 days of incubation, as shown in Figure 1(b). At 10 mL concentration of extract, the characteristic absorption peak is observed at 438 nm in UV-Vis spectrum which confirmed the formation of AgNPs and their stability on the 30th day (Figure 1 (b)). According to the generalized theory, only a single SPR band peak is expected in the absorption spectra of spherical nanoparticles, whereas anisotropic nanostructures or aggregates of spherical nanoparticles could give rise to two or more SPR bands depending upon the shape of the particles.⁴³

Morphology. The surface morphology of AgNPs was investigated at the microscale level, using FESEM with EDAX, and at the nanoscale level, using an HR-TEM. The formation of AgNP and its agglomeration can be observed at the microscale level (Figure 2(a)). The FESEM micrograph shows a spherical shape with a particle diameter that ranges from 5–23^onm. In particular, the average projected equivalent diameter⁴⁴ of AgNPs is 14 ± 9 nm. This number is validated by analyzing the sample at the nanoscale level. In Figure 2(b) and (c), it is clear that AgNPs produced by MP are spherical; the average aspect ratio is 1.09.

Chemical composition. AgNPs, regardless of the procedure used for the production, are supposed to show a strong aluminum peak in X-ray spectra. As expected, the presence of silver in the EDAX spectrum confirms the presence of elemental silver. The only elements detected using a FESEM-EDAX are aluminum or copper, oxygen, and silver. Aluminum (Al) and copper (Cu) are due to the aluminum foil and copper TEM grids used as substrate,

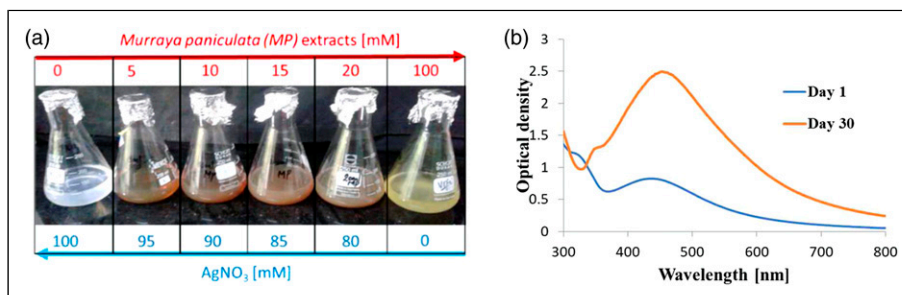


Figure 1. (a) Synthesis of silver nanoparticles using different concentrations of aqueous extracts from leaves of *M. paniculata* and different concentrations of AgNO₃. (b) UV-Vis spectrum of 10 mL of AgNPs solution at different times, 1 and 30 days.

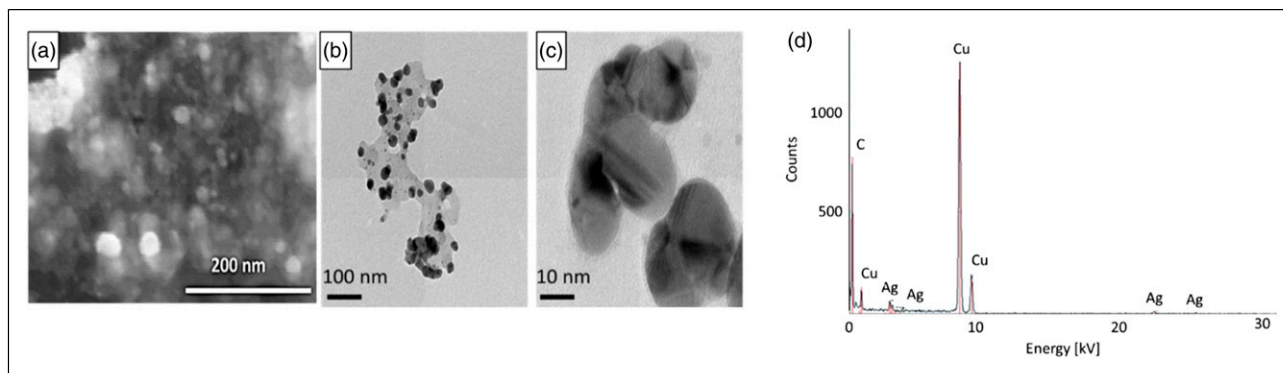


Figure 2. Examples of AgNPs generated from *M. paniculata* extract. The image is shown in (a) is obtained using an SEM, in (b) and (c) using an HR-TEM. In (d), an example of an EDAX analysis on AgNPs produced from leaves of *M. paniculata* is reported.

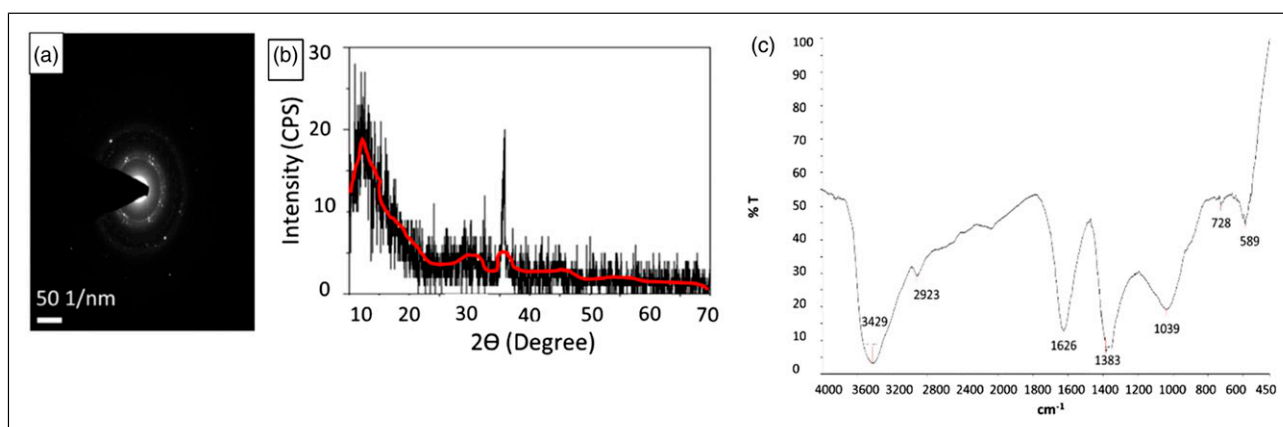


Figure 3. SAED (a) and X-Ray diffraction (XRD) (b) analysis of AgNPs from *M. paniculata*. In (d), an example of FTIR analysis of AgNPs from leaves of *M. paniculata* is shown.

respectively. Considering the above-mentioned elements and oxygen, silver shows an atomic percentage of about 30% with a standard deviation of 2 when analyzing three samples. Figure 2 (d) shows an example of an EDX sample where silver peaks are typical; metallic silver nanoparticles typically showed an absorption peak at 3 keV due to the surface plasmon resonance.⁴⁵

Solid-state. The crystallinity of AgNPs generated from MPs is analyzed by observing SAED patterns and deconvoluting an XRD spectrum. In Figure 3(a), the SAED patterns obtained by analyzing AgNPs produced from MP extract show a high crystallinity. The same conclusions can be reached by observing the XRD spectrum, Figure 3(b). Several Bragg reflections with 2θ values of 38.0° , 44.1° , and 64.6° sets of lattice plan were observed which may be indexed to (111), (200), and (220) facets of silver, respectively, confirms the FCC crystalline structure. The values are in agreement with the JCPDS (Joint Committee on Powder Diffraction Standard) file No. 04-078.

An FTIR measurement can determine the biomolecules responsible for the reduction and capping of synthesized AgNPs. The sharp and strong different peaks are observed at 3429cm^{-1} (O-H stretch, H-bonded alcohols, phenols groups), 2923cm^{-1} (C-H stretch alkanes), 1626cm^{-1} (N-H bend 1° amine), 1583cm^{-1} (C-C stretch in-ring aromatic), 1039cm^{-1} (C-N stretch aliphatic amines), 728cm^{-1} (C-Cl stretch alkyl halides), and 589cm^{-1} (C-Br stretch alkyl halides), respectively (Figure 3(c)). The results indicated that the interaction of amino groups, keto, and aldehyde⁴⁶ is responsible for AgNP synthesis. These data indicate that the involvement of phenols, alkanes, amines, aromatic, aliphatic amines, and alkyl halides residues present in *MP* in the nanoparticles synthesis. As mentioned earlier, leaves of *MP* are a rich source of alkaloids, phenolics, flavonoids, polysaccharides, and proteins. It is well known that proteins can bind to AgNPs through either amino acids or cysteine residues in the protein,⁴⁷ and therefore stabilization of AgNPs by surface-bound proteins is possible. A similar observation is noticed in the biological synthesis of AgNPs using *Jatropha curcas* seed extract.⁴⁸

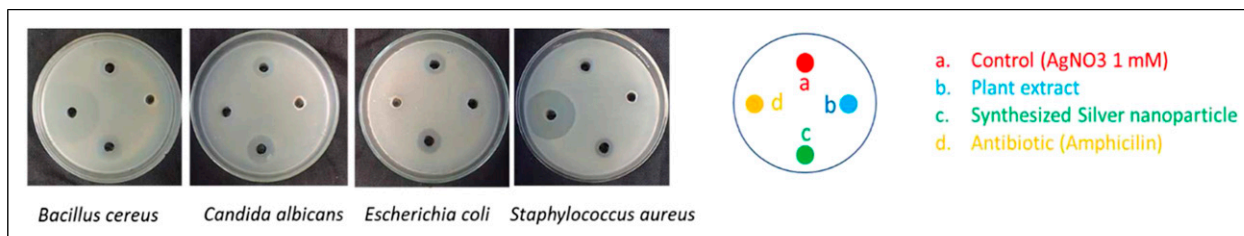


Figure 4. Antimicrobial activity of synthesized silver nanoparticles from leaves of *M. paniculata*.

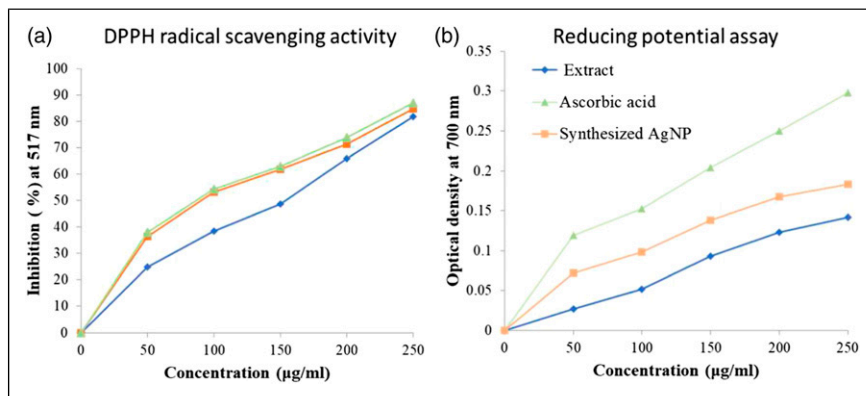


Figure 5. In (a), DPPH radical scavenging activity of synthesized silver nanoparticles from aqueous extract of *M. paniculata*. In (b), reducing the potential of synthesized silver nanoparticles from aqueous extract of *M. paniculata*.

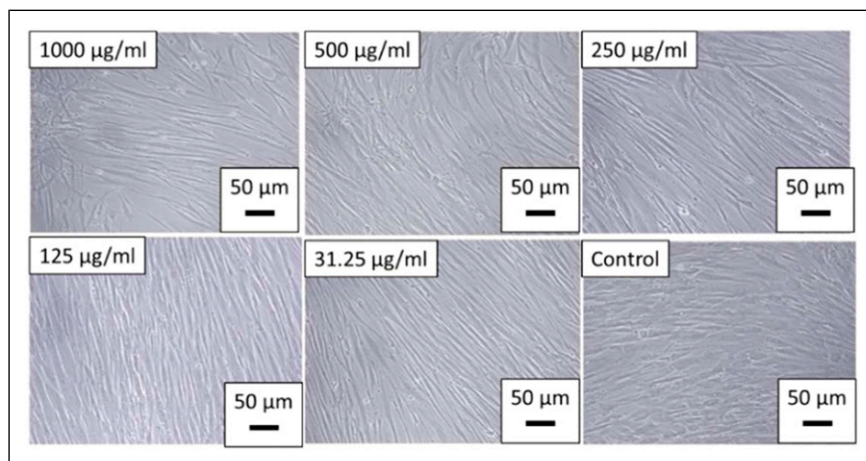


Figure 6. Cell viability of HUVEC by MTT assay and cytotoxicity were expressed as the concentration of 50% (IC50) cell growth inhibition. The experiments were performed in triplicates. Images were taken by Inverted Phase contrast microscope magnification $\times 20$ scale bar 50 μm .

Biological applications of silver nanoparticles

Antimicrobial activity. The synthesized AgNPs tested for their efficacy against human pathogens (*Staphylococcus aureus*, *Escherichia coli*, and *Candida albicans*). Our present study shows that the synthesized nanoparticles have potent activity against *Bacillus cereus* and *Candida albicans*

followed by *Escherichia coli* and *Staphylococcus aureus*. It shows that all the tested microorganisms were inhibited at the concentration of $100\ \mu\text{g/ml}$ of synthesized AgNPs. The antimicrobial activity of the aqueous extract, AgNPs, and standard drug was shown in Figure 4. The AgNPs show better activity against Gram-positive as compared to Gram-negative. The antimicrobial activities shown by AgNPs

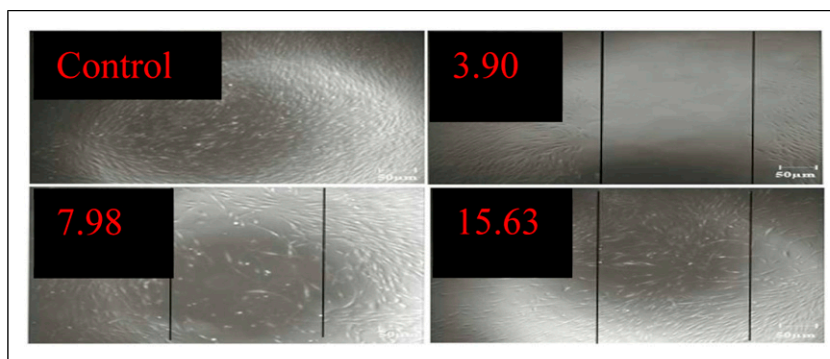


Figure 7. Cell migration potential by scratch wound assay. Photos were taken 48 hours after scratch wounding at $\times 4$ magnification.

synthesized using different plant systems may differ from species to species due to variations in shape and size of AgNPs, bacterial load, exposure time, and nutrient media.

The effects of AgNPs on bacterial cells are unclear and complicated.⁴⁹ However, there are various mechanisms on the action of AgNPs on the bacterial cell.⁵⁰ Some of these mechanisms were summarized and presented as follows: (i) the ability of AgNPs to anchor to the bacterial cell wall and then penetrate it,⁵¹ (ii) the formation of free radicals by the AgNPs which can damage the cell membrane and make it porous,^{52, 53} (iii) releasing the silver ions by the nanoparticles which can interact with the thiol groups of many vital enzymes and inactivate them,⁵⁴ and (iv) the nanoparticles can modulate the signal transduction in bacteria which stops the growth of bacteria.⁵⁵

All the human pathogens are resistant to standard drug ampicillin, but they are susceptible to the synthesized nanoparticle from leaves of *MP*. The results indicate that leaf extract alone did not exhibit antimicrobial activity against human pathogens. AgNO_3 (1 mM) shows an appreciable positive effect. However, plant AgNPs exhibit the greatest antimicrobial activity against tested human pathogens.

Antioxidant activity. In light of the difference among the wide range of assays available, a single antioxidant assay results can give only a reductive suggestion of the antioxidant potential. Moreover, the chemical complexity of samples with a mixture of different functional groups and chemical behavior could lead to a scattered result. Therefore, an approach with multiple assays in screening work is highly desirable. Thus, to better compare the results and cover a wide range of possible applications, *in vitro* antioxidant activities were assessed by different methods like reducing power and DPPH radical scavenging assay.

DPPH radical scavenging activity of AgNPs. Free radical scavenging activity is the most extensively used method to understand the potentiality of AgNPs toward their bioactivity. DPPH (purple) is a protonated radical which has a

characteristic absorbance at 517 nm using a spectrophotometer, which decolorizes (yellow) upon activation with antioxidants. Various researchers use DPPH scavenging activity as a fast and reliable parameter to assess the *in vitro* antioxidant activity of AgNPs solution. The DPPH scavenging activity of AgNPs increases in a dose-dependent manner (Figure 5(a)). The DPPH scavenging ability of the AgNPs is higher than the aqueous extract of *MP* and almost similar to that of standard ascorbic acid. Therefore, the AgNPs solution exhibits a proton-donating ability and could serve as a free radical inhibitor per scavenger, possibly acting as a primary antioxidant.

Reducing power assay using silver nanoparticles. Reducing power is associated with antioxidant activity,⁵⁶ and the compounds with reducing power indicate that they are electron donors and can reduce the oxidized intermediates of the lipid peroxidation processes; thus, they can act as primary and secondary antioxidants. The presence of antioxidants can result in the reduction of Fe^{3+} to Fe^{2+} , and the amount of Fe^{2+} complex is monitored by measuring the formation of blue color at 700 nm. The increased absorbance at 700 nm indicates an increase in reductive potential.

The reducing potential of synthesized AgNPs was found to surge with an increase in concentrations, indicating that the reducing potential of AgNPs was found to be lesser than that of the ascorbic acid (Figure 5(b)). It is evident from Figure 5 (b) that the reducing powers of the aqueous extract of *M. paniculata*, AgNPs, and the standard drug increase at high concentrations.

Cell viability assay using silver nanoparticles. The viability of HUVEC cells is checked using different doses (1000–3.906 $\mu\text{g}/\text{mL}$) of AgNPs from leaves of *MP*. At the concentration, 15.625 $\mu\text{g}/\text{mL}$ of AgNPs from *MP*, almost 89.03% of cells were viable (Figure 6). So, synthesized AgNPs from the *MP* do not show toxicity to HUVEC cells. It is toxic only when it exceeds the dosage level, that is, by increasing the concentration, AgNPs begin to show toxicity to the HUVEC cell line. Based on

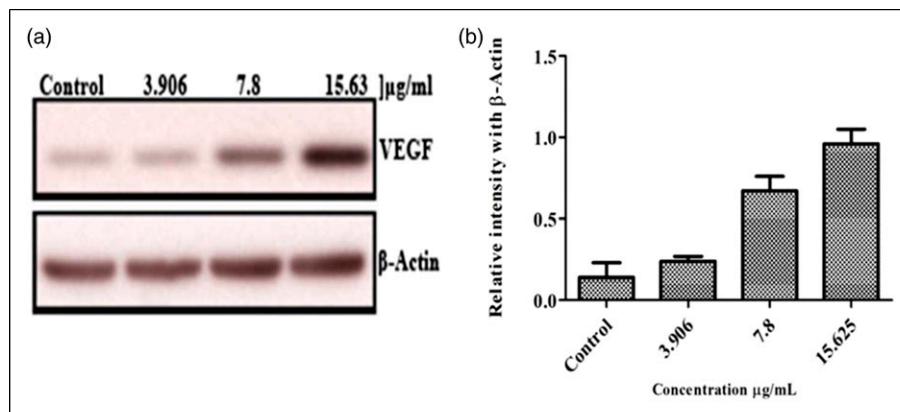


Figure 8. (a) Effect of silver nanoparticles from *M. paniculata* on the expression of VEGF in HUVEC cells and (b) quantitative expression of VEGF after normalization to β -actin.

this result, we conclude that AgNPs depicted angiogenic property by cell migration assay.

Cell migration assay using AgNPs. Angiogenesis is associated with several pathologies including cardiovascular diseases, chronic inflammation, cancer, and wound healing, and depending on the circumstances, it can be beneficial and deleterious. To explore the angiogenic potential of AgNPs from *MP*, HUVEC cells were treated with different concentrations of synthesized nanoparticles. At the concentration of $15.63\ \mu\text{g/ml}$, synthesized nanoparticles from *MP* enhance angiogenesis by cell migration after incubation for 48^ohours (Figure 7).

Wound healing involves the regeneration of specialized cells by the proliferation of surviving cells and connective tissue response characterized by the formation of granulation tissue.⁵⁷ It is also characterized by hemostasis, re-epithelialization, and remodeling of the extracellular matrix. Thus, the effect of ethanolic extract and the acetone fraction on wound contraction and epithelialization suggests it may enhance epithelial cell migration and proliferation, as well as the formation, migration, and action of myofibroblasts.

Expression of VEGF by western blotting analysis. VEGF is an important proangiogenic cytokine and improves angiogenesis during wound healing by stimulating the migration and proliferation of endothelial cells through the extracellular matrix.⁵⁸ The VEGF levels in HUVEC cells are up-regulated after 24 hours of incubation (Figure 8(a)). The highest upregulation of VEGF protein is detected at the concentration of $15.625\ \mu\text{g/ml}$ (Figure 8(b)).

Angiogenesis is a critical component in wound healing. Delayed or absent revascularization at the wound site contributes to the etiology of chronic wounds. Induction of angiogenesis by VEGF can be considered as a factor to improve wound healing. Western blotting analysis of HUVEC up-regulates the VEGF expression similar to that of β -actin.

Conclusion

Biosynthesizing nanoparticles are very common and have been extensively used in various biomedical applications. We developed a simple green chemistry approach for the synthesis of AgNPs by *MP* leaf extract. This approach demonstrates the multifunctional activities of biosynthesized AgNPs, which are mainly responsible for various secondary metabolites such as alkaloids, steroids, terpenoids, tannins, and other metabolites. We have observed the biocompatible nature of AgNPs toward the normal cells, and the results indicate the future application as a drug delivery vehicle to enhance angiogenesis. The synthesis of nanoparticles has several benefits, such as less toxicity, an eco-friendly approach, and cost-effectivity. Apart from that, biosynthesized AgNPs show enhanced antimicrobial activity compared to that of the standard drug. Besides, synthesized AgNPs show a good radical scavenging activity, which confirms that AgNPs have excellent antioxidant properties. We believe that biosynthesized AgNPs will open a new direction toward various biomedical applications in the future.

Acknowledgments

The authors greatly acknowledge the University Grant Commission (Grant Number GCCO/A-2/UGCBSR/2012/384 to P. Rama) and the Natural Sciences and Engineering Research Council of Canada (Grant Number RGPIN-2018-04735 to Anubhav Pratap-Singh) for financial support of this work. The authors are also thankful to the Director, CAS in Botany, University of Madras, Chennai, Tamil Nadu, India, for providing lab facilities.

Declaration of conflicting interests

The author(s) declared no potential conflicts of interest with respect to the research, authorship, and/or publication of this article.

Funding

The author(s) received no financial support for the research, authorship, and/or publication of this article.

ORCID iDs

Alberto Baldelli  <https://orcid.org/0000-0002-6296-5460>

Ammar B Altemimi  <https://orcid.org/0000-0001-7750-5988>

Anubhav Pratap-Singh  <https://orcid.org/0000-0003-1752-0101>

References

- Kuppusamy P, Yusoff MM, Maniam GP, et al.. Biosynthesis of metallic nanoparticles using plant derivatives and their new avenues in pharmacological applications - An updated report. *Saudi Pharm J* 2016; 24: 473–484.
- Baldelli A, Ou J, Li W, et al.. Spray-on nanocomposite coatings: wettability and conductivity. *Langmuir* 2020; 36: 11393–11410.
- Baldelli A, Ou J, Barona D, et al.. Sprayable, superhydrophobic, electrically, and thermally conductive coating. *Adv Mater Inter* 2021; 8: 1902110.
- Chaloupka K, Malam Y, and Seifalian AM. Nanosilver as a new generation of nanoparticle in biomedical applications. *Trends Biotechnol* 2010; 28: 580–588.
- Prow TW, Grice JE, Lin LL, et al.. Nanoparticles and microparticles for skin drug delivery. *Adv Drug Deliv Rev* 2011; 63: 470–491.
- Chaudhry Q and Castle L. Food applications of nanotechnologies: an overview of opportunities and challenges for developing countries. *Trends Food Sci Tech* 2011; 22: 595–603.
- Nair R, Varghese SH, Nair BG, et al.. Nanoparticulate material delivery to plants. *Plant Sci* 2010; 179: 154–163.
- Kelly FM and Johnston JH. Colored and functional silver nanoparticle–wool fiber composites. *ACS Appl Mater Inter* 2011; 3: 1083–1092.
- Govindan L, Anbazhagan S, Altemimi AB, et al.. Efficacy of antimicrobial and larvicidal activities of green synthesized silver nanoparticles using leaf extract of plumbago auriculata lam. *Plants* 2020; 9(11): 1577.
- Khan MAM, Kumar S, Ahamed M, et al.. Structural and thermal studies of silver nanoparticles and electrical transport study of their thin films. *Nanoscale Res Lett* 2011; 6: 434–438.
- Baldelli A, Bshaden B, Amirfazli A, et al.. Reproducibility of superhydrophobic and oleophobic polymeric micro surface topographies. *Surf Topography: Metrology Properties* 2020; 8(4): 045010.
- Hilger A, Cüppers N, Tenfelde M, et al.. Surface and interface effects in the optical properties of silver nanoparticles. *The Eur Phys J D* 2000; 10: 115–118.
- Chandra H, Patel D, Kumari P, et al.. Phyto-mediated synthesis of zinc oxide nanoparticles of berberis aristata: characterization, antioxidant activity and antibacterial activity with special reference to urinary tract pathogens. *Mater Sci Eng C* 2019; 102: 212–220.
- Nayak RR, Pradhan N, Behera D, et al.. Green synthesis of silver nanoparticle by penicillium purpurogenum NPMF: the process and optimization. *J Nanoparticle Res* 2011; 13: 3129–3137.
- Roy A, Bulut O, Some S, et al.. Green synthesis of silver nanoparticles: biomolecule-nanoparticle organizations targeting antimicrobial activity. *RSC Adv* 2019; 9: 2673–2702.
- Daniel SK, Banu BN, Harshiny M, et al.. Ipomea carnea-based silver nanoparticle synthesis for antibacterial activity against selected human pathogens. *J Exp Nanoscience* 2014; 9: 197–209.
- Park H, Hira SA, Muthuchamy N, et al.. Synthesis of silver nanostructures in ionic liquid media and their application to photodegradation of methyl orange. *Nanomater Nanotechnology* 2019; 9: 1847980419836500.
- Raji P, Samrot AV, Keerthana D, et al.. Antibacterial activity of alkaloids, flavonoids, saponins and tannins mediated green synthesised silver nanoparticles against Pseudomonas aeruginosa and Bacillus subtilis. *J Cluster Sci* 2019; 30: 881–895.
- Kalishwaralal K, Deepak V, Pandian SRK, et al.. Biosynthesis of silver and gold nanoparticles using Brevibacterium casei. *Colloids Surf B: Biointerfaces* 2010; 77: 257–262.
- Ranoszek-Soliwoda K, Tomaszewska E, Małek K, et al.. The synthesis of monodisperse silver nanoparticles with plant extracts. *Colloids Surf B: Biointerfaces* 2019; 177: 19–24.
- Collado A, Hernández G, Morejón V, et al.. Encapsulation of a Bioactive Steroid in a Polymer Matrix (Micro-encapsulation of DI-31 in Chitosan by Spray Drying for Various purposes) *Materials and Devices*, 2017.
- Liang H, Cao N, Zeng K, et al.. Coumarin and spirocyclopentenone derivatives from the leaves and stems of murraya paniculata (L.) Jack. *Phytochemistry* 2020; 172: 112258.
- Xiao P-G and Wang N-G. Can ethnopharmacology contribute to the development of anti-fertility drugs? *J Ethnopharmacology* 1991; 32: 167–177.
- Wu D, Lei Y, Tong Y, et al. Angiogenesis of the Frozen-thawed human fetal ovarian tissue at the early stage after xenotransplantation and the positive effect of salviae miltiorrhizae. *Anatomical Rec Adv Integr Anat Evol Biol* 2010; 293: 2154–2162.
- Rahman M, Hasanuzzaman M, Uddin N, et al.. Antidiarrhoeal and anti-inflammatory activities of murraya paniculata (L.) jack. *Pharmacologyonline* 2010; 3: 768–776.
- Bhardwaj M, Yadav P, Dalal S, et al.. A review on ameliorative green nanotechnological approaches in diabetes management. *Biomed Pharmacother* 2020; 127: 110198.
- Sharma P, Batra S, Kumar A, et al.. In vivo antianxiety and antidepressant activity of murraya paniculata leaf extracts. *J Integrative Medicine* 2017; 15: 320–325.
- Lotha R, Shamprasad BR, Sundaramoorthy NS, et al.. Biogenic phytochemicals (cassinopin and isoquercetin) capped copper nanoparticles (ISQ/CAS@CuNPs) inhibits MRSA biofilms. *Microb Pathogenesis* 2019; 132: 178–187.

29. Baldelli A, Trivanovic U, Sipkens TA, et al.. On determining soot maturity: a review of the role of microscopy- and spectroscopy-based techniques. *Chemosphere* 2020; 252: 126532.
30. Baldelli A, Trivanovic U, and Rogak SN. Electron tomography of soot for validation of 2D image processing and observation of new structural features. *Aerosol Sci Tech* 2019; 53: 575–582.
31. Baldelli A and Rogak SN. Morphology and Raman spectra of aerodynamically classified soot samples. *Atmos Meas Tech* 2019; 12.
32. Baldelli A, Esmeryan KD, and Popovicheva O. Turning a negative into a positive: trends, guidelines and challenges of developing multifunctional non-wettable coatings based on industrial soot wastes. *Fuel* 2021; 301: 121068.
33. Baldelli A, Trivanovic U, Corbin JC, et al.. Typical and atypical morphology of non-volatile particles from a diesel and natural gas marine engine. *Aerosol Air Qual Res* 2020; 20: 730–740.
34. Trivanovic U, Sipkens TA, Kazemimanesh M, et al.. Morphology and size of soot from gas flares as a function of fuel and water addition. *Fuel* 2020; 279: 118478.
35. Popovicheva O, Timofeev M, Persiantseva N, et al.. Microstructure and chemical composition of particles from small-scale gas flaring. *Aerosol Air Qual Res* 2019; 19: 2205–2221.
36. Kheirkhah P, Baldelli A, Kirchen P, et al.. Development and validation of a multi-angle light scattering method for fast engine soot mass and size measurements. *Aerosol Sci Tech* 2020; 54: 1–19.
37. Okeke MI, Iroegbu CU, Eze E, et al.. Evaluation of extracts of the root of *Landolphia owerrience* for antibacterial activity. *J Ethnopharmacology* 2001; 78: 119–127.
38. Blois MS. Antioxidant determinations by the use of a stable free radical. *Nature* 1958; 181: 1199–1200.
39. Oyaizu M. Studies on products of browning reaction. Antioxidative activities of products of browning reaction prepared from glucosamine. *Jpn J Nutr Diet* 1986; 44: 307–315.
40. Yue GG, Fan JT, Lee JK, et al.. Cyclopeptide RA-V inhibits angiogenesis by down-regulating ERK1/2 phosphorylation in HUVEC and HMEC-1 endothelial cells. *Br J Pharmacol* 2011; 164: 1883–1898.
41. Kittler S, Greulich C, Gebauer J, et al.. The influence of proteins on the dispersability and cell-biological activity of silver nanoparticles. *J Mater Chem* 2010; 20: 512–518.
42. Sönnichsen C, Reinhard BM, Liphardt J, et al.. A molecular ruler based on plasmon coupling of single gold and silver nanoparticles. *Nat Biotechnol* 2005; 23: 741–745.
43. Dwivedi P, Narvi SS, and Tewari RP. Phytofabrication characterization and comparative analysis of Ag nanoparticles by diverse biochemicals from *elaecarpus ganitrus* roxb., *terminalia arjuna* roxb., *pseudotsuga menzietii*, *prosopis spicigera*, *ficus religiosa*, *ocimum sanctum*, *curcuma longa*. *Ind Crops Prod* 2014; 54: 22–31.
44. Baldelli A, Boraey MA, Nobes DS, et al.. Analysis of the particle formation process of structured microparticles. *Mol Pharmaceutics* 2015; 12: 2562–2573.
45. Kaviya S, Santhanalakshmi J, Viswanathan B, et al.. Bio-synthesis of silver nanoparticles using citrus sinensis peel extract and its antibacterial activity. *Spectrochimica Acta A: Mol Biomol Spectrosc* 2011; 79: 594–598.
46. Yaylayan VA, Harty-Majors S, and Ismail AA. Monitoring carbonyl–amine reaction and enolization of 1-hydroxy-2-propanone (Acetol) by FTIR Spectroscopy. *J Agric Food Chem* 1999; 47: 2335–2340.
47. Gole A, Dash C, Ramakrishnan V, et al.. Pepsin–Gold colloid conjugates: preparation, characterization, and enzymatic activity. *Langmuir* 2001; 17: 1674–1679.
48. Bar H, Bhui DK, Sahoo GP, et al.. Green synthesis of silver nanoparticles using latex of *Jatropha curcas*. *Colloids Surfaces A: Physicochemical Eng Aspects* 2009; 339: 134–139.
49. Kim S-H, Lee H-S, Ryu D-S, et al.. Antibacterial activity of silver-nanoparticles against *Staphylococcus aureus* and *Escherichia coli*. *Microbiol Biotechnol Lett* 2011; 39: 77–85.
50. Prabhu S and Poulouse EK. Silver nanoparticles: mechanism of antimicrobial action, synthesis, medical applications, and toxicity effects. *Int Nano Lett* 2012; 2: 1–10.
51. SonDI I and Salopek-Sondi B. Silver nanoparticles as antimicrobial agent: a case study on *E. coli* as a model for gram-negative bacteria. *J Colloid Interf Sci* 2004; 275: 177–182.
52. Danilczuk M, Lund A, Sadlo J, et al.. Conduction electron spin resonance of small silver particles. *Spectrochimica Acta Part A: Mol Biomol Spectrosc* 2006; 63: 189–191.
53. Kim JS, Kuk E, Yu KN, et al.. Antimicrobial effects of silver nanoparticles. *Nanomedicine: Nanotechnology, Biol Med* 2007; 3: 95–101.
54. Feng QL, Wu J, Chen GQ, et al.. A mechanistic study of the antibacterial effect of silver ions on *Escherichia coli* and *Staphylococcus aureus*. *J Biomed Mater Res* 2000; 52: 662–668.
55. Shrivastava S, Bera T, Roy A, et al.. Characterization of enhanced antibacterial effects of novel silver nanoparticles. *Nanotechnology* 2007; 18: 225103.
56. Oktay M, Gülçin İ, and Küfrevioğlu Öİ. Determination of in vitro antioxidant activity of fennel (*Foeniculum vulgare*) seed extracts. *LWT - Food Sci Tech* 2003; 36: 263–271.
57. Whaley K and Burt A. Inflammation, healing and repair. *Muir's Textbook Pathol* 1996; 13: 112–165.
58. Ferrara N. Molecular and biological properties of vascular endothelial growth factor. *J Mol Med* 1999; 77: 527–543.